Reversible Surface Melting of PE and PEO Crystallites Indicated by TMDSC

Wenbing Hu,*,† Thomas Albrecht, and Gert Strobl

Faculty of Physics, Freiburg University, Hermann-Herder-Street 3, D-79104 Freiburg, Germany

Received June 2, 1999; Revised Manuscript Received August 26, 1999

ABSTRACT: Quasi-isothermal temperature-modulated differential scanning calorimetry was employed in a study of thermoreversible structural changes in the melting range of semicrystalline polymers. The results indicated a reversible melting and crystallization process occurring at the fold surfaces of crystallites of polyethylene and poly(ethylene oxide). For polyethylene, good agreements were found with reported small-angle X-ray scattering data and Fischer's theory. Surface melting and crystallization depend on the ability of the chains in the crystals to carry out a sliding diffusion. This was shown by a comparison of polyethylene and poly(ethylene oxide) with other polymers such as poly(ethylene terephthalate), polycaprolactone, isotactic polypropylene, and syndiotactic polypropylene. When the longitudinal chain mobility in the crystals is much reduced or completely absent, only a small or no excess reversing heat capacity is observed. The special performance of short-chain poly(ethylene oxide) is indicative for the metastability of the crystals built of once-folded chains.

I. Introduction

As a first-order phase transition, melting and crystallization are not reversible because supercooling is always needed for crystal growth. But this may not always be the case for the polymer crystallites due to their metastability; i.e., they will melt below the equilibrium melting point while the crystal growth is still possible. This reversibility can be further studied in recent years, since thermal analysis techniques were developed by employing a periodical modulation (usually sinusoidal) to the temperature, as the so-called temperature-modulated differential scanning calorimetry (TMDSC) measurement.[1] In this measurement, the thermal response (heat flow) is divided into an underlying part and a dynamic part, and the dynamic part is approximately expressed as a first-harmonic form of the temperature modulation with an amplitude A_{hf} and a phase lag θ (i.e., $A_{hf}\cos(\omega t - \theta)$, ω the modulation frequency). Then the reversing heat capacity of the sample can be obtained from the amplitude A_{hf}. Here, "reversing" just means that the thermal response is recovered in one period of the temperature modulation. With this experimental definition, the reversing heat capacity was observed in the melting range of polymer crystallites by conventional TMDSC measurement.[1] It was explained as an indication to the recrystallization behavior in the melting process. The melting−recrystallization behavior together with the sliding diffusion of the chains in the crystals has been considered to be the way of the crystal thickening during annealing.[2] Nevertheless, the thickening behavior of the lamellar crystallites is still irreversible; its contribution to the reversing heat capacity will relax down to zero during a long-time isothermal annealing.

In DSC measurement, the heat capacity contains two kinds of contributions: one is the thermodynamic heat capacity generated by the local thermal vibration of the atoms, and the other is the excess heat capacity generated by the thermal behaviors such as melting and crystallization. If we assume that the sample is only made up of crystalline and amorphous phases, the basic thermodynamic heat capacity can be calculated according to its linear dependence with the crystallinity α,

$$C_p(\text{thermodynamic}) = C_p(\text{crystalline})\alpha + C_p(\text{amorphous})(1-\alpha) \quad (1)$$

After long-time isothermal annealing, if all the irreversible processes like the melting−recrystallization process is finished and there is not any reversible process, the measured reversing heat capacities should be equal to the basic thermodynamical heat capacities. However recently, in the melting range of semicrystalline polymers, an additional reversing heat capacity above the basic thermodynamical values has been observed by quasi-isothermal measurement of TMDSC.[3,4] It shows a smooth transition from melting to crystallization in each cycle of temperature modulation[5] and does not really relax down to zero with a long-time annealing.[6] That implies a reversible thermal response of the semicrystalline polymers in the melting range, and its source from thermodynamical or excess contributions needs to be further studied. In fact, the reversible melting and crystallization of polyethylene crystallites on the fold surface[7] have been observed by SAXS measurement.[8] It will contribute to the reversible thermal response of the crystallites. In this paper, quasi-isothermal TMDSC measurement for a series of semicrystalline polymers is performed. The direct relationship between the additional reversing heat capacity and the reversible premelting behavior of the polymer crystallites will be demonstrated.

II. Experimental Details

A. Samples. The short-chain poly(ethylene oxide) (PEO) was purchased from Merck E., Darmstadt. The molar mass is 1000 Da. The long-chain PEO has average molar mass near 300 000 Da with a wide molar mass distribution. High-density polyethylene (PE) was supplied by Hoechst AG. The number of branches is less than 3 CH_3 per 1000 carbon atoms along

† On leave for Department of Macromolecular Science,Fudan university, 200433, Shanghai, P. R. China.

* To whom correspondence should be addressed.

10.1021/ma9908649 CCC: $18.00
Published on Web 10/15/1999

the backbone chain, and its weight-average molecular weight is about 390 000 with a wide molar mass distribution. Polypropylene samples with high tacticity were synthesized in the Institute of Macromolecular Chemistry of our university.[9] The syndiotactic sample (sPP) contains 3% meso-diads, and its weight-averaged molecular weight is 104 000, with the polydispersity index 1.7. The isotactic sample (iPP) contains >99% m sequences and >98% mmmm sequences, and its weight-averaged molecular weight is 54 400, with the polydispersity index 1.7. Poly(ethylene terephthalate) (PET) and poly(ϵ-caprolactone) (PCL) were purchased from Aldrich Chem. Co. (series number 20,025-5 and 18,160-9).

B. Apparatus. The Perkin-Elmer DSC4 apparatus with liquid-nitrogen cooling accessory was used. The sinusoidal oscillation of the temperature was generated by a software of ifa GmbH in Ulm, and the trigger rate was set as 50 data points per 100 s.

C. Quasi-Isothermal Measurement. In quasi-isothermal TMDSC measurement, the sample temperature T was set as a fixed mean temperature T_0 plus a small pertubation with a frequency ω ($=2\pi/p$, the period p is set as 60 s as a normal value) and an amplitude A_T (the normal value is 0.5 K):

$$T = T_0 + A_T \sin(\omega t) \tag{2}$$

The reversing heat capacity can be calculated from the amplitude of heat flow A_{hf} at a stationary state after long time annealing such as 30 min and the baseline of the empty pan measurement subtracting,

$$C_p(\text{reversing}) = \frac{A_{hf}}{\omega A_T} K \tag{3}$$

Here, K is a calibration constant, which has been found to be determined by the heat conduction constants, the modulation frequency, and the heat capacity of the empty pan.[10]

Within a modulation cycle, if there is no contribution of excess heat capacity, like in the melt state, the thermodynamic heat capacity of the sample should be measured as the reversing heat capacity. The calibration constant can thus be obtained according to the reported thermodynamic heat capacity of the melt state in the ATHAS databank.[11] Furthermore, this calibration constant was approximately fitted to the whole temperature range of measurements for the same sample.

To let the measurements cover the whole melting range of the sample, the mean temperature was increased or decreased stepwise after quasi-isothermal annealing to construct a heating or cooling process. The step length depends on the temperature region of interest. The jumping rate of the mean temperature is 5 K/min.

As a typical program for each sample, we first perform a slow cooling process as stated above from the melt state, followed with a heating process back to the melt state, and second take a temperature jump to the lowest point of the above process with a rate of 150 K/min, followed with a heating process back to the melt state. In these two heating processes, the performances of the samples with different thermal history can be compared.

III. Results and Discussion

A. Long-Chain Molecules. Short-chain molecules have been found to perform quite differently for the additional reversing heat capacities from the long-chain molecules in the heating process of the quasi-isothermal TMDSC measurement,[4] so we report this case in section D.

The reversing heat capacities of the long-chain samples in the typical program of quasi-isothermal measurement are shown in Figures 1−3. The samples can be classified into three groups according to their appearance in the heating process after a slow cooling (the cross points in Figures 1−3). The first group includes PE (Figure 1a) and long-chain PEO (Figure 1b), which shows a large reversing heat capacity in the melting range (C_p(maximum)/C_p(melt) > 1.2); the second group includes PET (Figure 2a), PCL (Figure 2b), and iPP (Figure 2c), which shows a small additional contribution (C_p(maximum)/C_p(melt) ∼ 1.1); the third group just includes sPP (Figure 3) and shows almost no additional reversing heat capacity in the melting range after a slow cooling.

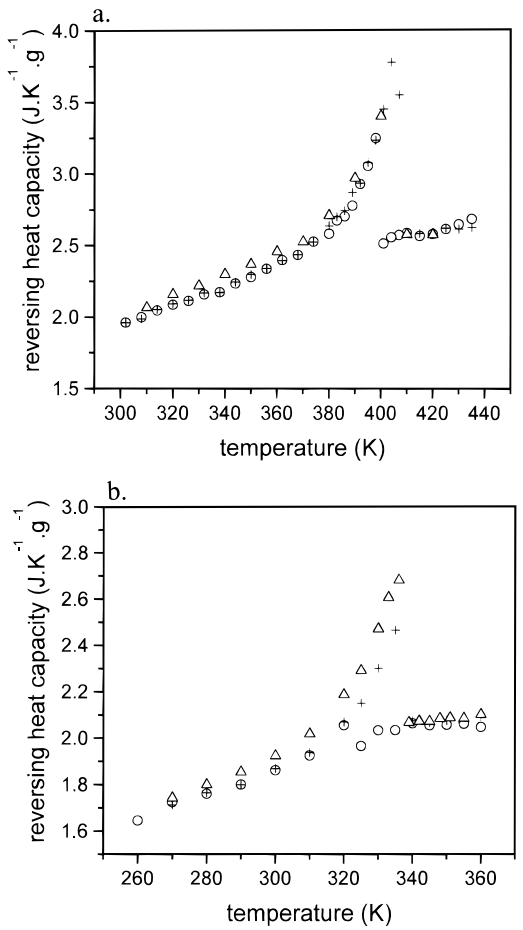

Figure 1. Quasi-isothermal TMDSC measurement for PE (a) and long-chain PEO (b). The circles refer to the slow cooling process, the crosses to the heating process after a slow cooling, and the triangles to the heating process after a fast cooling.

It is of interest to note that this classification corresponds to the ability of sliding diffusion of the molecules in the crystals. In the first group, PE and PEO are well-known for the effect of sliding diffusion to the lamellar thickening during annealing,[2] whereas for sPP, there is nothing like the dynamical mechanical α-process,[12] i.e., no c-slip process in the crystals. One can thus conclude that the additional reversing heat capacity may correspond to an additional thermal behavior, whose appearance is related to the sliding diffusion of the chains in the crystals.

Larger additional reversing heat capacities can be observed for all the samples in the heating process after fast cooling (the triangle points in Figures 1−3), but the heating process is not the only way to show the additional contribution. For PE, the cooling curve (the cycle points in Figure 1a) also shows the additional reversing heat capacity once the crystals form. This implies that the additional reversing heat capacity may be an intrinsic property of polymer crystals. Other long-chain samples, such as PEO, need so large supercooling to start crystallization that the additional contribution

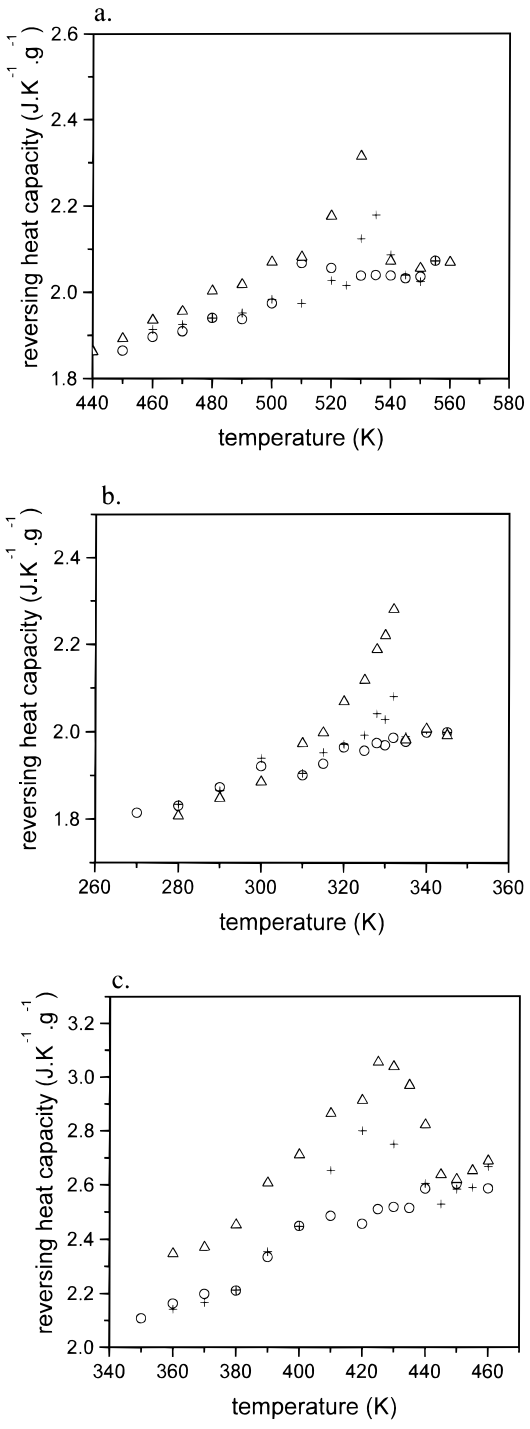

Figure 2. Quasi-isothermal TMDSC measurement for PET (a), PCL (b), and iPP (c). The circles refer to the slow cooling process, the crosses to the heating process after a slow cooling, and the triangles to the heating process after a fast cooling.

cannot be clearly observed during cooling. For PE, the additonal reversing heat capacity is rather stable when annealing for a long time (see Figure 4), like the reported observation for PET.[6]

Figure 5 shows the phase lag measured for the heating process of PEO after a slow cooling without baseline subtraction. The phase lag in the melt state is almost equal to that in the lower temperature region. This phase lag is mainly caused by the well-known heat conduction hindrance in the measuring system. After subtraction of this phase lag, the additional phase lag can be obtained which shows not only the heat flow

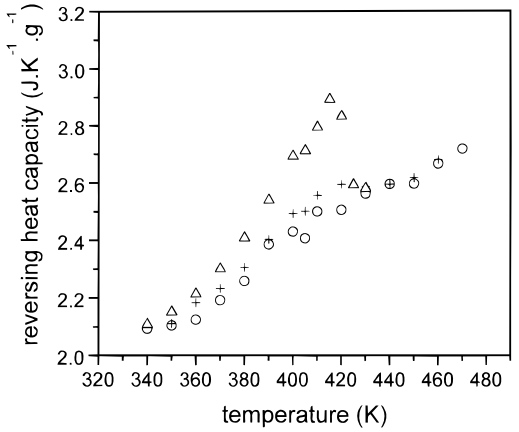

Figure 3. Quasi-isothermal TMDSC measurement for sPP. The circles refer to the slow cooling process, the crosses to the heating process after a slow cooling, and the triangles to the heating process after a fast cooling.

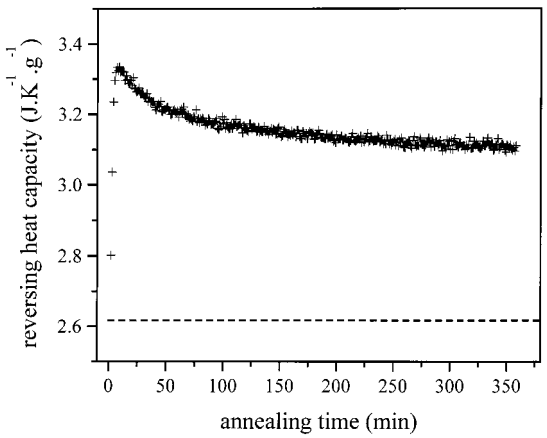

Figure 4. Change of the reversing heat capacity of PE with the time at a mean temperature of 395 K (crosses). The dashed line indicates the heat capacity of the melt state at 420 K.

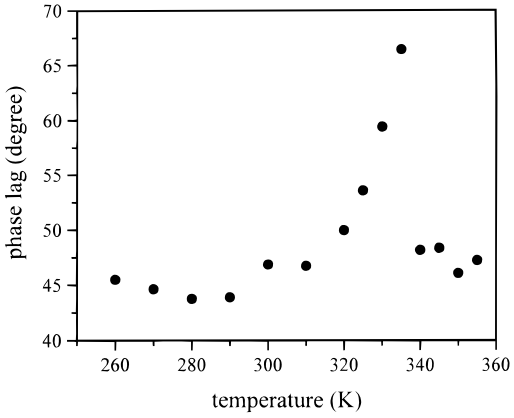

Figure 5. Phase lag of the heat flow observed for the long-chain PEO in the heating process after a slow cooling.

amplitude dependence but also the sample dependence. Obviously, this additional phase lag arises from the excess heat flow exchanged with the sample.

The additional reversing heat capacity is not very sensitive to the typical setting of the temperature modulation (period 60 s, amplitude 0.5 K). This is true at least for the case of PE cooling from 420 to 395 K with the rate 5 K/min and annealing at the end mean temperature. When choosing periods above 60 s, the ratio of the reversing heat capacity in the semicrystal-

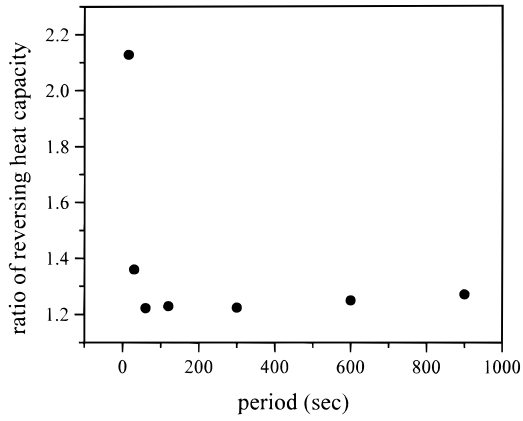

Figure 6. Ratio of the reversing heat capacity of PE at 395 K to that at 420 K for various periods of the temperature modulation. The modulation amplitude is fixed at 0.5 K.

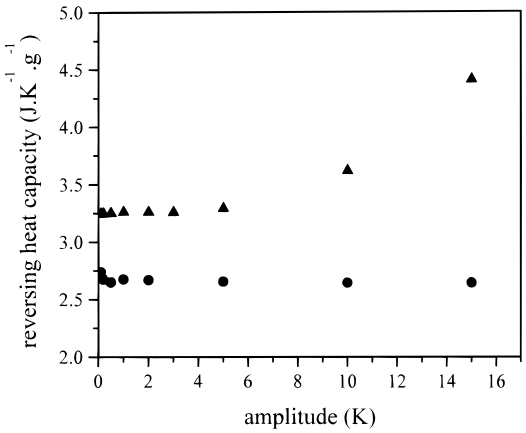

Figure 7. Reversing heat capacity of PE observed for different amplitudes of the temperature modulation, at 395 K (triangles) and 420 K (circles). The period of modulation is fixed at 60 s.

line state to that in the melt state remains constant (see Figure 6). Below the period of 60 s, a deviation from the constant ratio was observed which may be attributed to the nonlinear effect of the heat conduction hindrance in the measuring system, but the direction of this deviation is still an open question. When keeping the amplitude of modulation below 5 K, no change in the value of reversing heat capacity occurs (see Figure 7). Compared with the melt state, the large increase of the reversing heat capacity of the semicrystalline state occurs above the amplitude 5 K. This is a consequence of an additional melting−recrystallization process because the large amplitude has covered the temperature gap between the melting and the crystallization of the same crystallites. As have been reported for the similar case of indium,[5] a distortion of ellipse in the Lissajous figure (heat flow vs temperature curve) occurs with larger amplitude (see Figure 8); i.e., there is a small melting peak in the heating cycle as well as a small negative crystallization peak in the cooling cycle. This additional thermal behavior is reversing in each cycle but not reversible. Below an amplitude of 5 K, Lissajous figures are just smooth ellipses which imply a reversible thermal behavior for the additional reversing heat capacity.

The explanation for the reversible additional reversing heat capacity in the melting range may start from two directions corresponding to the contributions of the heat capacity in DSC measurement. The first is the thermodynamic heat capacity of the atoms located in

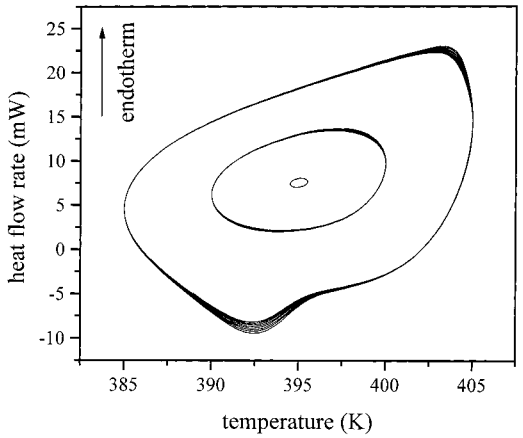

Figure 8. PE at 395 K: Lissajous figures registered for the modulation amplitudes 0.5, 5, and 10 K, respectively. The period of temperature modulation is fixed at 300 s.

the defects and the surface region of the crystallites. But it was not observed in the lower temperature region (see Figure 10 or ref 13), and up to now, we have no evidence for its so strong temperature dependence in the melting range.

The second is the excess heat capacity contributed by reversible melting and crystallization on an active surface. Principally, the active surface may be the lateral surface as well as the fold surface for the lamella crystallites. On the lateral surface, the melting point of crystallites depends on the thickness of the lamella, while at the same temperature, recrystallization on the lateral surface always generates thicker lamella. So this process will be irreversible and unstable with a long-time annealing; the only exception for this case is very near to the melting point of the most stable crystals when the amplitude of the temperature modulation is large enough to cover the gap between the melting and the crystallization,[5] but the ellipse in Lissajous figure will be distorted. So the best explanation for the above observations is the reversible premelting behavior of polymer crystals on the fold surface.[7]

For long-chain molecules, crystallization from the melt state will always produce metastable folded-chain crystals with a large amount of loops and tie molecules on the fold surface.[14] Fischer[15] has proposed a reasonable model to explain the reversible premelting behavior on the fold surface, according to the force balance between the recovery tendency of the stretched loops to draw the stem out of crystals and the tendency of lamellar thickening to draw the loops into crystals. Changing the temperature just moves the position of the balance together with the fold surface and leads to the reversible change in crystallinity. Quantitative comparison with our TMDSC data will be given in the next section. However, this model has not yet clearly described how the sliding diffusion of the chains in the crystals plays its role in this local balance.

On heating, thermal expansion of the crystalline chains along the transverse direction cannot supply sufficient free space for the partial melting on the fold surface. The disorder conformation on the fold surface can exist just because the lamella contains enough number of sharp or neighboring foldings to avoid surface crowding.[16] Only when a large number of sharp fold ends go back into the crystal and produce free space on the fold surface, the fold surface melting becomes possible. The going back of the sharp fold ends can be

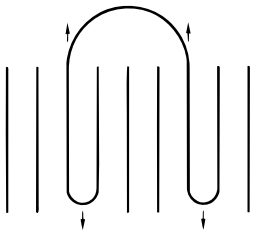

Figure 9. Schematic plot of the local force balance between the recovery tendency of the stretched loops and the thickening tendency of the lamella (see arrows).

realized through the sliding diffusion, when the other end of the stem is a stretched loop with recovery tendency, as schematically shown by the up arrows in Figure 9. This is usually the case in the melt-crystallized folded-chain crystallites, where the fold surface mainly consists of the loops and the sharp foldings. On cooling, the sharp fold end will tend to go ahead to stabilize the thickness of the lamellae; meanwhile, the loop ends will be drawn into the crystals and the loops stretch again (the down arrows in Figure 9). So a local force balance between the recovery tendency of the stretched loops and the thickening tendency of the lamella will temporarily exist only through the sliding diffusion of the chains in the crystals.

The crystallization in a fast cooling process may generate more defects in the crystals, more stretched loops on the fold surface, and more thin lamellae. They all favor the sliding diffusion in the crystals and the local premelting behavior. Therefore, even in the heating process of sPP after a fast cooling, the reversible premelting may still be realized locally (see the triangle points in Figures 1−3).

B. Comparison of Excess Heat Capacities of PE with Fischer's Theory. Quantitative comparison of the excess reversing heat capacities due to the premelting behavior is possible, if we subtract the basic thermodynamic heat capacity of the sample from the reversing heat capacity at each annealing temperature. The crystallinity can be obtained from the area of the melting peak in conventional DSC measurement with scanning-up rate 20 K/min after annealing. The results of the excess reversing heat capacity of PE are shown in Figure 10.

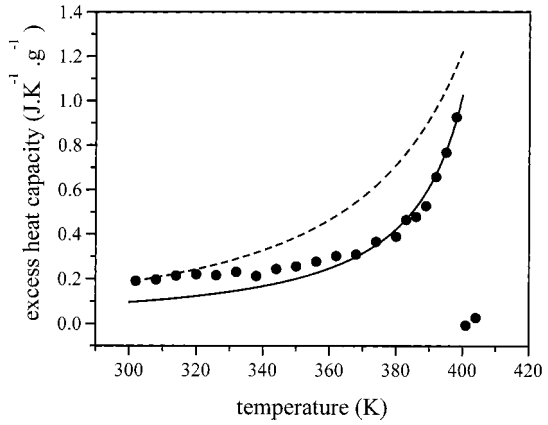

Figure 10. Excess reversing heat capacities observed for PE during cooling (the filled circles). The solid line is the theoretical prediction from Fischer's model, and the dashed line is calculated from the smoothed result of SAXS measurement.

The theoretical calculation based upon Fischer's model is only effective for the polymers with high crystallinity, because the amorphous phase was assumed to be constructed only by the loops. The loops (n segments with length b) are treated as Gaussian chains; their ends are fixed at a distance R, so their partition function is

$$P(R^2,n) = Z^n\left(\frac{2\pi nb^2}{3}\right)^{-3/2} \exp\left(-\frac{3R^2}{2nb^2}\right) \qquad (4)$$

Here, Z^n is the partition function of the same chain without constraints. If the amorphous phase is assumed to be made up of ν loops, its free energy is

$$G_a = -\frac{\nu}{\beta}\ln P = \frac{\nu}{\beta}\left(n\beta\mu_a + \frac{3}{2}\ln\frac{2\pi b^2}{3} + \frac{3}{2}\ln n + \frac{3R^2}{2nb^2}\right) \qquad (5)$$

with

$$\beta\mu_a = -\ln Z \quad \left(\beta = \frac{1}{k_B T}\right)$$

in which μ_a is the chemical potential per segment in the amorphous phase. Assuming the number of segments in the amorphous phase $n_a = \nu n$, with the number of segments in the crystalline phase n_c and the chemical potential per segment in the crystalline phase μ_c, the total free energy G is the sum of the contributions from these two phases

$$G = n_c\mu_c + n_a\mu_a + \frac{3\nu}{2\beta}\left(\ln\frac{2\pi b^2}{3} + \ln n + \frac{R^2}{nb^2}\right) \qquad (6)$$

Under the condition $n_a + n_c =$ constant, the local equilibrium can be found by minimization of G for the loop length n. R^2 can be considered as the mean-square end-to-end distance of the free loops with an initial length n_0, so $R^2 = n_0 b^2$. The equilibrium loop length n_{eq} can thus be obtained from

$$\beta(\mu_a - \mu_c) = \frac{3(n_0 - n_{eq})}{2n_{eq}^2} \qquad (7)$$

with the approximated driving force for crystallization[17]

$$\beta(\mu_a - \mu_c) = \frac{H_m(T_m - T)}{k_B T_m^2}$$

Here H_m is the heat of fusion per segment, and T_m is the equilibrium melting point. The driving force for crystallization determines that n_{eq} is always smaller than its initial value n_0. This indicates the stretching state of the loops balanced with the tendency of crystallization. The result is

$$n_{eq} = s(\sqrt{1 + 2n_0/s} - 1) \qquad (8)$$

with

$$s = \frac{3k_B T_m^2}{4H_m(T_m - T)}$$

On the basis of the two-phase model of the semicrystalline polymers, the crystallinity can be expressed as

$$\frac{1-\alpha}{\alpha} = \frac{2un_{eq}m}{S\lambda\rho_c} \tag{9}$$

Here, u is the average number of the loops on each fold surface of the lamella, m is the mass per segment, S is the sectional area of the crystals along the fold surface, λ is the average thickness of the lamellae, and ρ_c is the density of the crystalline phase. On the fold surface, the sharp folding occupies about 30% of surface area,[18] while the loops occupy almost all the others. (The number of tie molecules and cilia is assumed to be small.) So $70\% \times S = 2uf$, where f is the transverse area per chain. Equation 9 becomes

$$\alpha = \frac{1}{1 + \dfrac{0.7n_{eq}m}{f\lambda\rho_c}} \tag{10}$$

For the case of PE in the slow cooling process, the crystallization starts at 398 K (see Figure 1a), while the average thickness of lamella λ has been found to be about 220 Å.[8] Like in ref 15, each segment contains six repeat units, $m = 6 \times 14$ g/mol, $f = 7.36 \times 4.92/2$ Å^2, $\rho_c = 1.0$ g/cm^3, $H_m = 6 \times 940$ cal/mol, and $T_m = 419$ K. Choosing $n_0 = 100$, we can thus calculate the heat capacity from

$$C_p = -\Delta H_m \frac{d\alpha}{dT} = -\Delta H_m \frac{d\alpha}{dn_{eq}} \frac{dn_{eq}}{dT} \tag{11}$$

where ΔH_m is the heat of fusion per gram of the crystals, 281.3 J/g. The results of the theoretical prediction for the excess reversing heat capacity are shown in Figure 10.

From Figure 10, we can clearly see that the excess reversing heat capacities of PE fit well with the theoretical prediction of the premelting behavior. The average initial loop length is about 100 segments. Its mean-square-root of end-to-end distance is 30.9 Å under the assumption of a Gaussian chain. This value is something larger than the "cluster correlation length" (16.9 Å) measured from the intermediate q range of neutron scattering according to the "widely spaced stem cluster" model.[19] This means that only long loops can supply enough entropy loss to balance with the driving force of crystallization. If the cluster model for the conformation of the whole chains in the semicrystalline state is acceptable, the reversible premelting can be considered as a result of the stretching recovery of both the long loops and the long tie molecules between the clusters, and the going-back of the sharp fold ends will cooperate over the whole range of each cluster through sliding diffusion.

C. Comparison of the Excess Heat Capacities of PE with the Results of SAXS Measurement. The surface premelting behavior of long-chain PE has been directly observed in the small-angle X-ray scattering (SAXS) measurement.[8] Over the whole temperature range, the crucial quantity—the specific inner surface O_s—remains constant in the vicinity of 0.065 nm^{-1}. On the basis of the two-phase model of the semicrystalline polymers, there exists the following relationship between the crystallinity α and the average thickness of the amorphous layers d_a,

$$1 - \alpha = \frac{O_s}{2} d_a \tag{12}$$

According to the shape of the reported data d_a vs temperatures, a function $d_a = c/(T_0 - T)$ was chosen to smooth the discrete data points. Thus, $1/d_a$ vs temperatures in the heating process can be regressed into the linear relation $1/d_a = T_0/c - T/c$ with a good correlation coefficient of 0.987 and $T_0 = 464$, $c = 549.45$. The excess heat capacity due to the premelting behavior was calculated as a smooth curve

$$C_p = -\Delta H_m \frac{d\alpha}{dT} = \Delta H_m \frac{O_s}{2} \frac{c}{(T_0 - T)^2} \tag{13}$$

The results are also shown in Figure 10.

From Figure 10, the results of these two measurements not only show a similar temperature dependence but also agree essentially in the absolute values. This comparison further supports our conclusion that the observed excess reversing heat capacities mainly originate from the premelting behavior of polymer crystallites on the fold surface.

D. Short-Chain Molecules. In the case of short-chain PEO, as shown in Figure 11, a peak of the reversing heat capacity occurs at the lower side of the melting range; its height depends on the thermal history. When the sample has crystallized in a fast cooling process, the peak is higher, and the time evolutions of the heat flow amplitude in the higher side of the peak region (305−309 K) show a change from increase to decrease (see Figure 12). This implies that a metastable state may exist below a critical temperature located in the vicinity of 307 K.

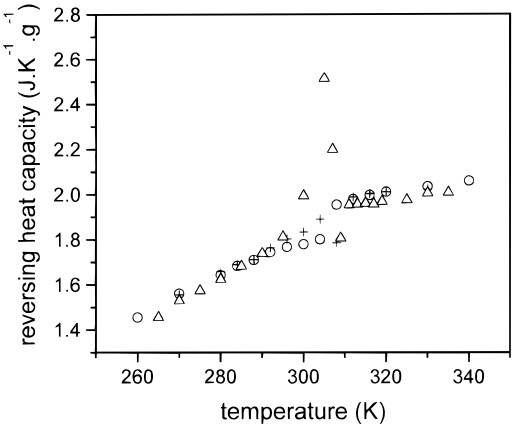

Figure 11. Quasi-isothermal TMDSC measurement for short-chain PEO. The circles refer to the slow cooling process, the crosses to the heating process after a slow cooling, and the triangles to the heating process after a fast cooling.

It is well-known that, in a fast cooling process from the melt state, short-chain PEO will tend to form metastable folded-chain crystals, while the most stable extended-chain crystals can form only in a slow cooling process. The initial folding in the metastable crystals is rather irregular; the lamella will perform thickening to the extended-chain crystals as well as thinning to the once-folded-chain crystals during the isothermal annealing.[20] If we consider the additional reversing heat capacity as an intrinsic property of the once-folded-chain

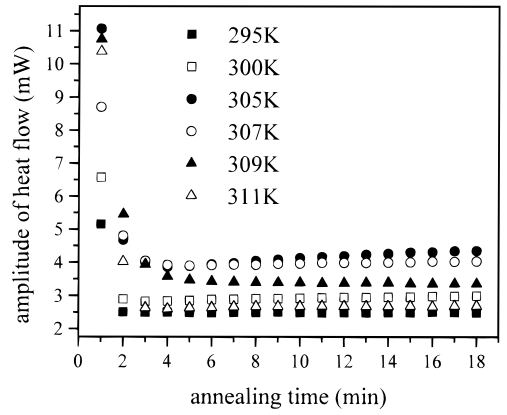

Figure 12. Change of the amplitude of the heat flow rate with time at different mean temperatures registered for short-chain PEO after fast cooling.

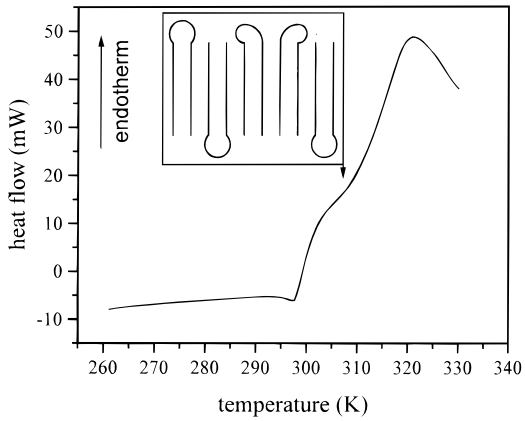

Figure 13. Conventional DSC curve measured for short-chain PEO after a fast cooling (heating rate: 50 K/min). The shoulder can be assigned to the melting of the once-folded-chain crystals drawn in the inset.

crystals, its weak appearance in the heating process after a slow cooling (the cross points in Figure 11) can be explained according to few metastable crystals forming in this case, while in the heating process after a fast cooling, the increase tendency of its values with time evolution can be explained as the increase of the amount of metastable crystals due to lamellar thinning. In fact, one can observe the melting point of this metastable crystal in conventional DSC measurement; as indicated in Figure 13, it is located in the vicinity of 307 K.

The once-folded-chain crystals can perform reversible premelting on the fold surface because the sharp folding does not favor the local conformational energy at the fold end. If the space on the fold surface permits, the fold end will expand (see the inset plot in Figure 13). So within a limit of expansion the sharp fold ends will always tend to draw the stem out of the crystals if it is not balanced by the crystal growth tendency along the stems. A local equilibrium may thus be established between the thermodynamic relaxation of the fold ends and the thickening tendency of the lamella. It contributes to the reversible excess heat capacity in the melting range of the metastable crystallites.

IV. Conclusion

On the basis of a series of quasi-isothermal TMDSC measurements, the additional reversing heat capacity observed in the melting range of PE and PEO crystallites is assigned to an excess contribution of reversible premelting on the fold surface both for long-chain molecules and for short-chain molecules. The sharp folding and the stretched loops contribute to the high surface free energy of the lamellar crystals, so the premelting is just a result of the relaxation tendency of the surface free energy. As a necessary prerequisite, a sliding diffusion of the chains in the crystallites has to be activated. Since this reversible contribution to the reversing heat capacities is stable over long time, one can distinguish it from those irreversible contributions such as the lamellar thickening through a melting−recrystallization process or a sliding diffusion in the solid state.

Acknowledgment. W.H. thanks Mr. Christoph Schick in Rostock University and Dr. Werne Stille, Dr. Reinhard Sigel, Dr. Masanori Iijima, and Mrs. Silvia Siegenführ in our group for helpful discussions. The stipendium of the graduate college 'Strukturbildung in Makromolekularen Systemen' at Freiburg University is also appreciated by W.H.

References and Notes

(1) Reading, M. *Trends Polym. Sci.* **1993**, *8*, 248−253.
(2) Fischer, E. W. *Pure Appl. Chem.* **1972**, *31*, 113−131.
(3) Okazaki, I.; Wunderlich, B. *Macromolecules* **1997**, *30*, 1758−1764.
(4) Ishikiriyama, K.; Wunderlich, B. *Macromolecules* **1997**, *30*, 4126−4131.
(5) Wunderlich, B.; Okazaki, I.; Ishikiriyama, K.; Boller, A. *Thermochim. Acta* **1998**, *324*, 77−85.
(6) Schick, C.; Merzlyakov, M.; Wunderlich, B. *Polym. Bull.* **1998**, *40*, 297−303.
(7) Strobl, G. *The Physics of Polymers*, 2nd ed.; Springer: Berlin, 1997; p 185.
(8) Albrecht, T.; Strobl, G. *Macromolecules* **1995**, *28*, 5827−5833.
(9) Thomann, R.; Wang, C.; Kressler, J.; Jüngling, S.; Mülhaupt, R. *Polymer* **1995**, *36*, 3795−3801.
(10) Wunderlich, B.; Jin, Y.; Boller, A. *Thermochim. Acta* **1994**, *238*, 277−293.
(11) See ATHAS Database on WWW (Internet), URL: http://funnelweb.utcc.utk.edu/∼athas.
(12) Sakata, Y.; Unwin, A. P.; Ward, I. M. *J. Mater. Sci.* **1995**, *30*, 5841−5849.
(13) Wunderlich, B. *Macromolecular Physics;* Academic Press: New York, 1973; Vol. 1, p 403.
(14) Flory, P. J. *J. Am. Chem. Soc.* **1962**, *84*, 2857−2867.
(15) Fischer, E. W. *Kolloid Z. Z. Polym.* **1967**, *218*, 97−114.
(16) Frank, F. C. *Discuss. Faraday Soc.* **1979**, *68*, 7−13.
(17) Hoffman, J. D. *J. Chem. Phys.* **1958**, *29*, 1192−1193.
(18) Jing, X.; Krimm, S. *J. Polym. Sci., Polym. Lett.* **1982**, *21*, 123−125.
(19) Fischer, E. W. *Makromol. Chem., Makromol. Symp.* **1988**, *20/21*, 277−291.
(20) Cheng, S. Z. D.; Zhang, A.; Barley, J. S.; Habenschuss, A.; Zschack, P. R. *Macromolecules* **1991**, *24*, 3937−3944.

MA9908649